

Slow-light dispersion properties of multiatomic multiband coupled-resonator optical waveguides

Sunkyu Yu, Xianji Piao, and Namkyoo Park*

Photonic Systems Laboratory, School of EECS, Seoul National University, Seoul 151-744, Korea

(Received 23 November 2011; revised manuscript received 31 January 2012; published 21 February 2012)

In this paper, we investigate the dispersion properties of a multiatomic coupled-resonator optical waveguide (CROW), and show the existence of band-dependent group velocities in its slow-light bands. By including the next-nearest-neighbor coupling terms in a coupled-mode theory (CMT) analysis for the structure, we explain the physical origin of the band-dependent group velocities in terms of the modification of molecular mode-coupling strengths, and also derive the criteria for complete band separation and perfect intermode intensity overlap. Our results imply that when estimating the performance of a multiwave slow-light device, the band dependency of group velocities must also be considered in addition to the conventional CROW dispersion. Numerical analysis with a photonic crystal platform shows excellent agreement with theory.

DOI: [10.1103/PhysRevA.85.023823](https://doi.org/10.1103/PhysRevA.85.023823)

PACS number(s): 42.70.Qs, 42.82.Et, 42.79.Gn

I. INTRODUCTION

Slow-light structure [1–3] has been considered to be one of the key elements for future all-optical functional devices. Many notable advantages of slow light, such as its larger group index, small footprint, and reduced power operation have been demonstrated in various forms [4–8]. In particular, with the orders-of-magnitude enhancement of optical nonlinearities—derived from light compression in the spatial domain [7–10], it now became possible to seriously consider the option of optical signal processing, which has been difficult to achieve with conventional structures or materials. For instance, a slow-light enhanced nonlinear phase shift has been used to construct power-efficient and compact all-optical modulators [7,10], tunable buffers [11], parametric conversions [12], and optical analog-to-digital converters [13,14].

Still, while modern wavelength-division multiplexed systems and most of all-optical signal processing devices require more than one wave (for example, control, signal, and clock), the slow-light structures, in general, have been designed for single-band operation [1–13] and have rarely been extended to incorporate multiband, multichannel functionalities [14–16]. As an example, for an all-optical, high-speed logic device based on cross-phase modulation (XPM) [17,18], a multiband slow-light coupled-resonator optical waveguide (CROW) with perfect intensity overlap and matched group velocities of its bands would be ideal.

In this paper, in order to extend our understanding of slow-light structures, we study the dispersion properties of a multiband multiatomic CROW, using coupled-mode theory (CMT) supported by a numerical assessment. To incorporate the interference between multiatomic molecular field patterns into the slow-light coupling strength, next-nearest-neighbor interaction terms are included in the CMT analysis of the multiatomic CROW structure. By assessing the results of the CMT, a simple formula describing the origin of the band-dependent dispersion for each multiatomic (MA)-CROW band is derived. The physical origin of the band-dependent group velocity is then explained in terms of the modification of the molecular mode-coupling strength, which is the result of

the mode-dependent interference from next-nearest-neighbor couplings. The result of our analysis implies that the performance limitation of multiatomic CROW devices has to be estimated by including mode-dependent group velocity, which has been ignored in the past, rather than using only the conventional CROW time-bandwidth relation [19]. The criteria for band separation and intermode intensity overlap are also discussed. Numerical assessments using a photonic crystal MA-CROW and all-optical slow-light travelling-wave Mach-Zehnder switch show excellent agreement with the analytical solution developed from the coupled-mode theory.

II. THEORY: BAND-DEPENDENT DISPERSION OF A MULTIATOMIC CROW

To study the slow-light operation of a multiatomic CROW, coupled-mode theory [20,21] is employed. The MA-CROW unit cell is composed of multiples of single-mode atomic cavities, each at a resonant frequency of ω_0 , that are tightly coupled together with an internal coupling coefficient κ_i (Fig. 1). When isolated, the unit cell forms a resonator molecule having orthogonal modes of nondegenerate frequency. The nearest-neighbor coupling between the atoms in neighboring molecules is also represented by an external coupling coefficient κ_o . It is critical to note that the current analysis includes a *cross-coupling coefficient* κ_c between next-nearest-neighbor resonators (dashed lines in Fig. 1), which has been neglected in previous studies [14,16]. Under this arrangement, field amplitudes a_k^m ($m = 1 \sim n$, with n representing the number of atomic resonators in the k th molecule) can be written in a matrix form:

$$\frac{dA_k}{dt} = -i\omega_0 I_n A_k + i\kappa_i C_n A_k + i\kappa_o I_n (A_{k-1} + A_{k+1}) + i\kappa_c C_n (A_{k-1} + A_{k+1}), \quad (1)$$

where A_k is the vector with its m th component being the field amplitude of the m th atomic resonator in the k th molecule ($[A_k]_m = a_k^m$), I_n is the $n \times n$ identity matrix, and C_n is the $n \times n$ matrix denoting the next-nearest-neighbor couplings ($[C_n]_{pq} = 1$ for $|p-q| = 1$, $[C_n]_{pq} = 0$ otherwise).

Now, by applying Bloch-wave harmonic functions $a_k^m = A_{+m} e^{-i\omega t + ik\beta\Lambda} + A_{-m} e^{-i\omega t - ik\beta\Lambda}$ (β being the propagation constant and Λ is the distance between molecules) with a

*nkpark@snu.ac.kr

periodic boundary condition, a governing equation for the dispersion relations for n -atomic CROW can be obtained:

$$M_n A_k = O, \quad (2)$$

where the matrix M_n is

$$M_n = \begin{bmatrix} (\omega - \omega_0) + 2\kappa_o \cos(\beta\Lambda) & \kappa_i + 2\kappa_c \cos(\beta\Lambda) & 0 & \cdots & 0 \\ \kappa_i + 2\kappa_c \cos(\beta\Lambda) & (\omega - \omega_0) + 2\kappa_o \cos(\beta\Lambda) & \kappa_i + 2\kappa_c \cos(\beta\Lambda) & \cdots & 0 \\ 0 & \kappa_i + 2\kappa_c \cos(\beta\Lambda) & (\omega - \omega_0) + 2\kappa_o \cos(\beta\Lambda) & \cdots & 0 \\ \vdots & \vdots & \vdots & \ddots & \vdots \\ 0 & 0 & 0 & \kappa_i + 2\kappa_c \cos(\beta\Lambda) & (\omega - \omega_0) + 2\kappa_o \cos(\beta\Lambda) \end{bmatrix}. \quad (3)$$

As can be clearly seen, M_n now represents the nearest- and next-nearest-neighbor couplings altogether. It is worth noting that by setting the diagonal and off-diagonal elements to $\Omega = (\omega - \omega_0) + 2\kappa_o \cos(\beta\Lambda)$ and $K = \kappa_i + 2\kappa_c \cos(\beta\Lambda)$, M_n can be rewritten as $M_n = \Omega I_n + K C_n$. In order to get the dispersion relations, we first derive a recurrence relation for the determinant of M_n :

$$\det(M_n) = \Omega \det(M_{n-1}) - K^2 \det(M_{n-2}). \quad (4)$$

Applying the initial conditions of $n = 1$ [atomic CROW, $\det(M_1) = \Omega$] and $n = 0$ [null space, $\det(M_0) = 1$], we can now write down the determinant of M_n for n -atomic CROW as follows:

$$\det(M_n) = \frac{2^{-(n+1)}}{\sqrt{\Omega^2 - 4K^2}} [(\Omega + \sqrt{\Omega^2 - 4K^2})^{n+1} - (\Omega - \sqrt{\Omega^2 - 4K^2})^{n+1}]. \quad (5)$$

Setting $\det(M_n) = 0$ to get nontrivial solutions, we can then obtain the following relation:

$$\frac{\Omega + \sqrt{\Omega^2 - 4K^2}}{\Omega - \sqrt{\Omega^2 - 4K^2}} = e^{i[2p\pi/(n+1)]}, \quad (6)$$

where p is an integer ($1 \leq p \leq n$). The closed-form expression for Ω can then be obtained:

$$\Omega = \frac{1 + e^{i[2p\pi/(n+1)]}}{e^{i[p\pi/(n+1)]}} K = 2K \cos \frac{p\pi}{n+1}. \quad (7)$$

At this point, it is worth noting the functional form of the matrix $M_n = \Omega I_n + K C_n$. While ΩI_n describes the dynamics of isolated *atomic* CROW (coupled by κ_o), the off-diagonal elements of $K C_n$ describe the rest of the interactions in MA-CROW. Meanwhile both the κ_i and $2\kappa_c \cos(\beta\Lambda)$ terms in

K contribute to the modification of the eigenvalues of the molecular modes, and it is critical to mention that *only the cross-coupling-originated $2\kappa_c \cos(\beta\Lambda)$ term* [with a nonzero β differential $\partial K/\partial\beta \sim 2\kappa_c \Lambda \sin(\beta\Lambda)$] *modifies the group velocity*.

To get further insight into the effect of the cross-coupling κ_c to the dispersion properties of multiatomic CROW, we now calculate explicitly the dispersion relation and group velocity. Substituting the functional forms of Ω and K into Eq. (7), we finally arrive at n sets of dispersion relations and group velocities ($p = 1 \sim n$),

$$\omega_p = \omega_0 + 2\kappa_i \cos \frac{p\pi}{n+1} - 2 \left(\kappa_o - 2\kappa_c \cos \frac{p\pi}{n+1} \right) \cos \beta\Lambda, \quad (8)$$

$$v_{gp} = 2 \left(\kappa_o - 2\kappa_c \cos \frac{p\pi}{n+1} \right) \Lambda \sin \beta\Lambda. \quad (9)$$

As can be seen from the dispersion equations (8) and the triatomic example in Fig. 2, after the introduction of a nonzero κ_c , the *functional forms* of the n dispersion curves start to deviate from each other [Figs. 2(a), 2(b), and Eq. (8)] depending on the *band number* p .

This band number p -dependent deviation of dispersion curves then leads to differences in their group velocities [Fig. 2(c) and Eq. (9)], which would otherwise ($\kappa_c = 0$) be solely determined by κ_o [1]. To note, in practical applications, the cross-coupling strength κ_c will be dependent on both δ and Λ (Fig. 1); meanwhile κ_i and κ_o will be dependent only on δ and Λ , respectively. It is worth mentioning, by comparing Figs. 2(a) and 2(b) it is easy to see that complete band separation can be achieved only for a regime of strong internal coupling. From Eq. (8), we derive the criteria for band separation between the $p-1$ th and p th band as

$$|\kappa_i| > 2 \left| \frac{\kappa_o - \left(\cos \frac{p}{n+1} \pi + \cos \frac{p-1}{n+1} \pi \right) \kappa_c}{\cos \frac{p}{n+1} \pi - \cos \frac{p-1}{n+1} \pi} \right|. \quad (10)$$

Before examining dispersion properties of MA-CROW as a function of n (number of atoms in a molecule), it is better to understand the physical origin of the band-dependent group velocity. The case of a diatomic CROW is illustrated in Fig. 3(a). Compared to single-atom CROW (where dispersion curves are determined by κ_o alone), the *effective coupling strengths* between diatomic *molecules* come to have different

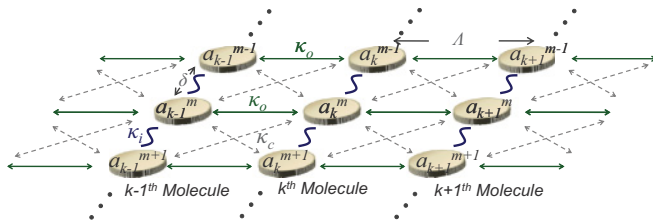


FIG. 1. (Color online) Coupled-mode theory model of a multiatomic, multiband CROW. $\kappa_{i,o,c}$: coupling constants between resonators; a_k^m : field amplitude in the m th atomic resonator in molecule k .

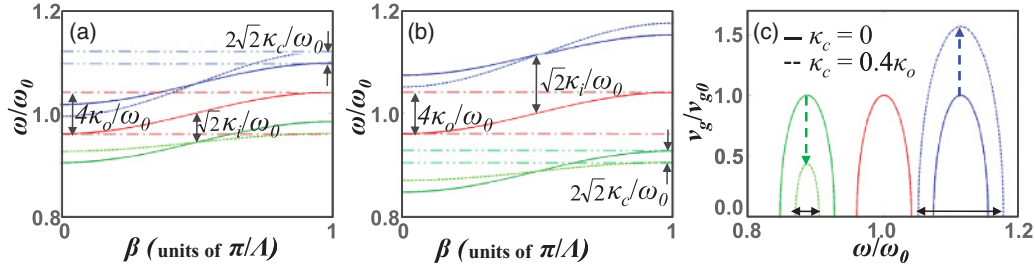


FIG. 2. (Color online) Dispersion curves of a triatomic CROW in (a) a weak internal coupling regime ($\kappa_i = -0.04\omega_0$, $\kappa_o = 0.02\omega_0$) and (b) a strong internal coupling regime ($\kappa_i = -0.08\omega_0$, $\kappa_o = 0.02\omega_0$). Effect of cross coupling is evident by comparing $\kappa_c = 0$ (solid line) and $\kappa_c = 0.4\kappa_o$ (dashed line). (c) Group velocities for the dispersion curves in (b). Group velocities are normalized to v_g ($\omega = \omega_0$, $\kappa_c = 0$).

values depending on the molecular-mode field patterns—that is, constructive or destructive interference between κ_o and κ_c (red and black arrows) directly affect the effective coupling. Similarly, for n -atomic molecules, the effective coupling between molecules [$\kappa_{\text{eff}} = \kappa_o - 2\kappa_c \cos[p\pi/(n + 1)]$, from Eq. (9)] comes to have different values depending on the mode field pattern (or band number p), in addition to being affected by the number of atoms, n , in a molecule. Figure 3(b) shows the calculated group velocities as a function of atomic number n , at the band centers, v_g [$\beta = 0.5(\pi/\Lambda)$, $\kappa_c = 0.2\kappa_o$]. The deviation of group velocities for n -atomic CROW modes, from that of isolated ($n = 1$) CROW modes increases with n , up to a limit of $2(\kappa_o \pm 2\kappa_c)\Lambda$ (in the case of all- constructive or destructive interaction between κ_o and κ_c).

III. IMPLICATIONS IN DEVICE PERFORMANCES: GROUP VELOCITY WALK-OFF EFFECT

To investigate the implications of these findings for device applications, as an example here we estimate the system penalty from the group velocity walk-off [22–24], in cross-phase modulation devices. In the presence of signal-control walk-off, the limit of the nonlinear phase shift φ for the signal is given by [25]; $\varphi < \Delta k L_w \approx \Delta k [\Delta T / (1/v_g^{\text{signal}} - 1/v_g^{\text{control}})]$, where Δk is the XPM-induced wave-vector change, L_w is the walk-off length, and ΔT is the pulse width. Restricting the present analysis to cases of maximum XPM efficiency [i.e., p and q modes of identical $|\mathbf{E}(x, y)|^2$, $p + q = n + 1$ as shown

in Fig. 3(c)], now for a device using the p th (q th) band as a signal (control) wave for all-optical modulation, the walk-off limited device bandwidth $\Delta\omega$ then can be easily estimated, using $\Delta\omega \sim 1/\Delta T$ in φ and Eq. (9):

$$\Delta\omega < \Delta\rho_{\text{XPM}} \frac{\sigma\omega_0}{\varphi v_{gp}} \left| \frac{1}{v_{gp}} - \frac{1}{v_{gq}} \right|^{-1} = \Delta\rho_{\text{XPM}} \frac{\sigma\omega_0}{\varphi} \frac{\kappa_o}{4\kappa_c \cos \frac{p\pi}{n+1}}, \tag{11}$$

where $\Delta\rho_{\text{XPM}}$ is the XPM-induced nonlinear refractive index change ratio, ω_0 is the signal frequency, and σ is the mode energy fraction in the nonlinear region [7].

The blue lines in Fig. 4(a) show the bandwidth (device speed) limit of a multiatomic CROW device. With the increase of cross coupling κ_c , the walk-off (11) becomes the dominant factor in the bandwidth limit of the device, and gives values far below those determined by the CROW dispersion only [19] [red line in Fig. 4(a)]. It is worth noting that the maximum bandwidth penalty is weakly dependent on the atomic number n , and saturates at a value proportional to $\kappa_o/(4\kappa_c)$, as expected from the maximum and minimum group velocities of $2(\kappa_o \pm 2\kappa_c)\Lambda$ [Fig. 3(b)]. To verify our theory, we utilize multiatomic CROWs on a photonic crystal platform. By assuming a two-dimensional square-lattice, rod-type photonic crystal of lattice constant $a = 528$ nm, rod index $n_{\text{rod}} = 3.5$, and radius $r = 0.2a$, CROWs made of point defect resonators ($r_d = 0.07a$, $\Lambda = 3a \sim 6a, \delta = 2a \sim 3a$) are constructed. Figures 4(b) and

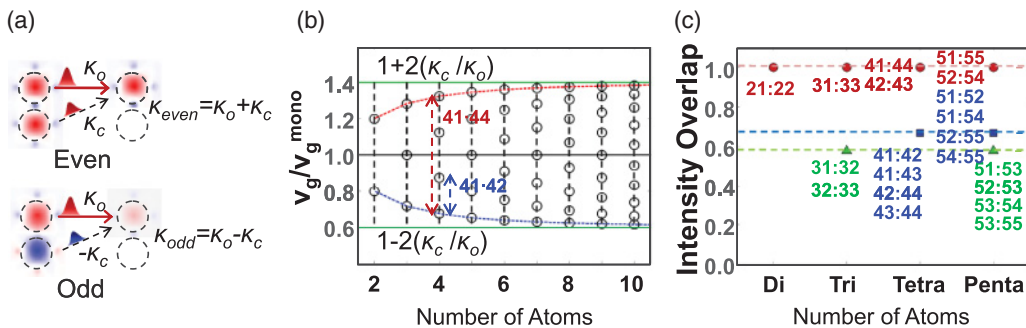


FIG. 3. (Color online) (a) Band-dependent modification of molecular coupling strength for a diatomic CROW; from constructive (even mode, $\kappa_{\text{even}} = \kappa_o + \kappa_c$) and destructive (odd mode, $\kappa_{\text{odd}} = \kappa_o - \kappa_c$) interferences. (b) Deviations in group velocity for each molecular mode, plotted for different n -atomic molecules. κ_c was set to $0.2\kappa_o$. v_g^{mono} denotes the group velocity of single-atom CROW. (c) Intensity overlap between molecular modes p and q (marked as $np:nq$). Perfect intensity overlap can be obtained if $p + q = n + 1$; for example, $p = 1$ and $q = 4$ for $n = 4$.

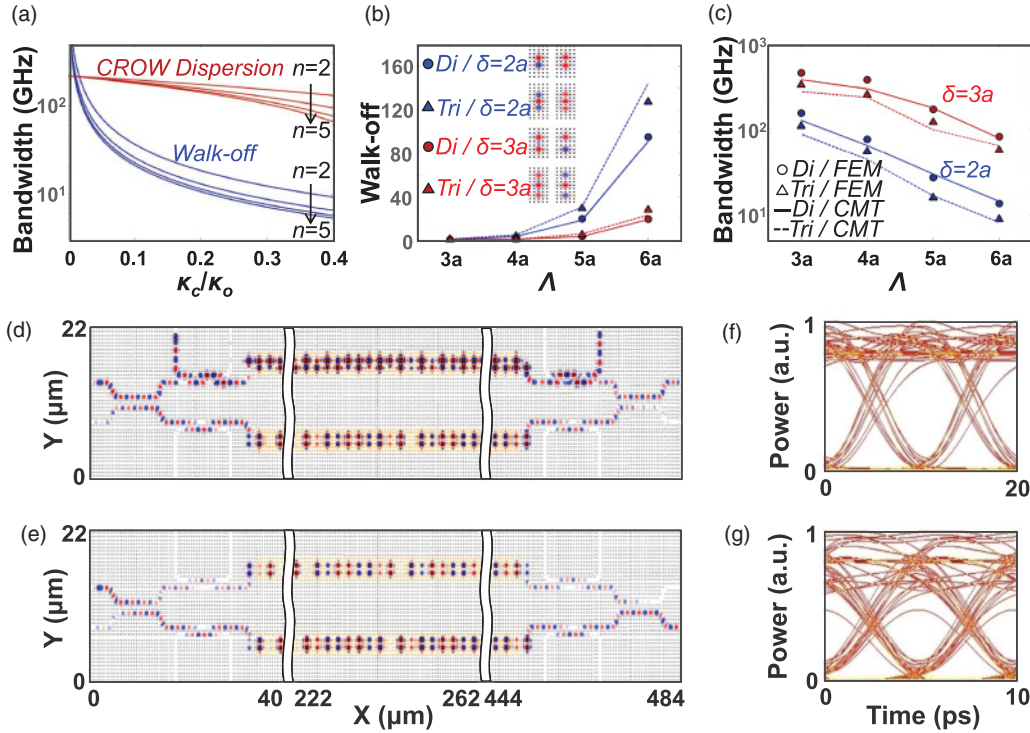


FIG. 4. (Color online) (a) Bandwidth limit of multiatomic CROW, for different cross-coupling coefficient κ_c . Blue and red lines show the walk-off- and CROW dispersion-limited bandwidth, respectively, for different MA-CROW structures ($n = 2-5$). A plot was made for the cases of $p = 1$ and $q = n$ by assuming maximum band separation and a perfect intensity overlap between the signal and control waves. $\Delta\rho_{\text{XPM}} = 0.02\%$, $\lambda_0 = 2\pi c/\omega_0 = 1550$ nm, $\sigma = 0.6$, $\varphi = \pi$, and $\kappa_o = 0.001\omega_0$. [(b), (c)] A plot of the theoretically (lines) and field-emission microscopy (FEM) calculated (symbols) (b) walk-off parameter $\Delta n_g = c|1/v_{gp} - 1/v_{gq}|$ and (c) bandwidth limit, for di- and triatomic CROWs ($\Lambda = 3a-6a$, for $\delta = 2a$ and $3a$). Coupling coefficients for the CMT analysis were calculated from the isolated resonator modes [20]. Switching operation of diatomic CROW MZI for (d) on state and (e) off state. Optical eye of the switched output, for pseudorandom bit sequence control waves at (f) 100 and (g) 200 Gbps.

4(c) show the group-velocity walk-off and walk-off limited bandwidth, respectively, for the constructed CROW. For the tested di- and also triatomic examples, excellent agreement between theory (CMT, lines) and numerical assessments (COMSOL, symbols) were observed, for different κ_o ($\sim\Lambda^{-1}$) and κ_c [$\sim(\Lambda^2 + \delta^2)^{-1/2}$]. Note that for a fixed value of δ , larger Λ results in increased walk-off and associated penalties, as the difference in strength between external coupling κ_o and cross coupling κ_c decreases.

As an application example of *multiband* slow-light structures, we constructed an all-optical travelling-wave Mach-Zehnder interferometer (MZI), which could be utilized for all-optical switching [10], analog-to-digital conversion [14], or parametric conversions [12,26]. To achieve an operation speed of ~ 100 GHz, and at the same time sufficient frequency separation between control and signal waves, diatomic CROWs of $\Lambda = 4a$ and $\delta = 2a$ were used [14]. A nonlinear Kerr index of $n_2 = 1.5 \times 10^{-17}$ m²/W was assumed in the modulation region, constructed with a diatomic CROW of 200 cascaded molecule resonators. For the analysis of the switching operation, a finite-difference time-domain (FDTD, two-dimensional) method [27] was employed. A continuous-wave (CW) input signal, with 100 and 200 Gbps modulated control waves (2^6-1 bits pseudorandom bit sequence, of third-order super-Gaussian nonreturn to zero pulses) was fed to the MZI to measure the bandwidth and output signal quality of

the all-optical switching action. Figures 4(d) and 4(e) show the slow-light enabled low-power (10 mW/ μ m for CW input, and maximum 30 mW/ μ m for control) switching action of the MZI. From the FDTD-generated optical eye [Figs. 4(f) and 4(g)], an optical signal quality factor Q of 9.6 was obtained for the 100 Gbps signal output. In contrast, at 200 Gbps [near the estimated walk-off bandwidth of ~ 70 GHz [Fig. 3(c)], much worse, marginally acceptable optical quality factors $Q = 3.5$ were observed, supporting the signal-control walk-off limited bandwidth analysis for MA-CROW.

Extending our understanding on slow-light structures, we revealed the existence and origin of the band-dependent dispersion in a multiatomic, multiband slow-light structures. By including next-nearest interactions in the CMT analysis of a multiatomic CROW, a clear derivation of the band-dependent dispersion equation was possible. An elucidation of its physical origin was made, in terms of the molecular field pattern interference between κ_o (external coupling between CROW molecules) and κ_c (cross coupling). By identifying conditions for complete band separation and also intensity overlap between different modes, our analysis provides guidelines in the design of multiwave slow-light devices, in photonic crystal, ring resonator, or plasmonic platforms. The implications of theoretical findings were elucidated in terms of the group velocity walk-off penalty, for an example of photonic crystal-based XPM devices. A perfect match between theory

and numerical analysis was found supporting the analysis that the performance of the multiatomic slow-light devices has to be estimated including the effect of molecular field patterns. Our analysis addressing the physical origin of the band-dependent group velocity can be envisioned in the future to devise a means of reducing detrimental cross-coupling effects—for example, by utilizing resonance modes of anisotropic profiles.

ACKNOWLEDGMENTS

This work was supported by the Global Research Laboratory Project (K20815000003) and in part by the Center for Subwavelength Optics (SRC, 2011-0001054), both funded by the Korean government through National Research Foundation.

-
- [1] A. Yariv, Y. Xu, R. K. Lee, and A. Scherer, *Opt. Lett.* **24**, 711 (1999).
- [2] Q. Gan, Y. J. Ding, and F. J. Bartoli, *Phys. Rev. Lett.* **102**, 056801 (2009).
- [3] M. Notomi, E. Kuramochi, and T. Tanabe, *Nature Photon.* **2**, 741 (2008).
- [4] Y. Saito and T. Baba, *Opt. Express* **18**, 17141 (2010).
- [5] J. B. Khurgin, *J. Opt. Soc. Am. B* **22**, 1062 (2005).
- [6] G. T. Purves, C. S. Adams, and I. G. Hughes, *Phys. Rev. A* **74**, 023805 (2006).
- [7] M. Soljačić, S. G. Johnson, S. Fan, M. Ibanescu, E. Ippen, and J. D. Joannopoulos, *J. Opt. Soc. Am. B* **19**, 2052 (2002).
- [8] M. Ebnali-Heidari, C. Monat, C. Grillet, and M. K. Moravvej-Farshi, *Opt. Express* **17**, 18340 (2009).
- [9] B. Corcoran, C. Monat, C. Grillet, D. J. Moss, B. J. Eggleton, T. P. White, L. O’Faolain, and T. F. Krauss, *Nature Photon.* **3**, 206 (2009).
- [10] K. Inoue, H. Oda, N. Ikeda, and K. Asakawa, *Opt. Express* **17**, 7206 (2009).
- [11] C. J. Chang-Hasnain, P. Ku, J. Kim, and S. Chuang, *Proc. IEEE* **91**, 1884 (2003).
- [12] J. B. Khurgin, *Phys. Rev. A* **72**, 023810 (2005).
- [13] S. Yu, S. Koo, and N. Park, *Opt. Express* **16**, 13752 (2008).
- [14] S. Yu, X. Piao, S. Koo, and N. Park, in *Microoptics Conference 2009* (Optical Society of Japan, Tokyo, 2009).
- [15] Z. Kang, W. Lin, and G. P. Wang, *J. Opt. Soc. Am. B* **26**, 1944 (2009).
- [16] I. Chremmos and O. Schwelb, *J. Opt. Soc. Am. B* **27**, 1242 (2010).
- [17] Y. J. Jung, C. W. Son, Y. M. Jhon, S. Lee, and N. Park, *IEEE Photon. Technol. Lett.* **20**, 800 (2008).
- [18] B. Olsson, P. Öhlén, L. Rau, and D. J. Blumenthal, *IEEE Photon. Technol. Lett.* **12**, 846 (2000).
- [19] S. Mookherjea, *Opt. Lett.* **30**, 2406 (2005).
- [20] H. A. Haus, *Waves and Fields in Optoelectronics* (Prentice-Hall, Englewood Cliffs, NJ, 1984).
- [21] C. Manolatou, M. J. Khan, S. Fan, P. R. Villeneuve, H. A. Haus, and J. D. Joannopoulos, *IEEE J. Quantum Electron.* **35**, 1322 (1999).
- [22] R. Danielius, A. Piskarskas, P. Di Trapani, A. Andreoni, C. Solcia, and P. Foggi, *Opt. Lett.* **21**, 973 (1996).
- [23] A. V. Smith, *Opt. Lett.* **26**, 719 (2001).
- [24] J. Huang, J. R. Kurz, C. Langrock, A. M. Schober, and M. M. Fejer, *Opt. Lett.* **29**, 2482 (2004).
- [25] G. P. Agrawal, *Fiber-Optic Communication Systems* (Wiley, New York, 2002).
- [26] Y. J. Ding and J. B. Khurgin, *IEEE J. Quantum Electron.* **32**, 1574 (1996).
- [27] A. Taflove and S. C. Hagness, *Computational Electrodynamics: The Finite-Difference Time-Domain Method* (Artech House, Boston, 2000).